Inorg. Chem. **1996,** *35,* 2981−2987

Heterometallic Alkoxides of Zirconium with Tin(II) or Lead(II)

Daniel J. Teff, John C. Huffman, and Kenneth G. Caulton*

Department of Chemistry and Molecular Structure Center, Indiana University,
Bloomington, Indiana 47405-4001

Received November 2, 1995[⊗]

Syntheses of $SnZr(OR)_6$ (R = ^iPr, ^tBu) and $PbZr(O^tBu)_6$ are described. With Pb and the smaller ligand O^iPr, no 1:1 compound forms, but instead $Pb_4Zr_2(O^iPr)_{16}$ and $Pb_2Zr_4(O^iPr)_{20}$ are isolated. The latter two compounds are shown to have serpentine (not *closo*) structures with six-coordinate Zr and three- and four-coordinate Pb. Spectroscopic studies show fluxionality (including Pb site exchange) and retention of structure in aromatic solvents. Synthetic interconversions are effected with addition of the appropriate alkoxide ($Pb(O^iPr)_2$ or $Zr(O^iPr)_4$) with the correct stoichiometry. Titanium forms no analogous compounds. Crystallographic data (both $P2_1/c$ at −174 °C) for $Pb_4Zr_2(O^iPr)_{16}$, $a = 12.190(6)$ Å, $b = 14.701(7)$ Å, $c = 19.978(13)$ Å, and $\beta = 105.57(3)°$ with $Z = 2$; for $Pb_2Zr_4(O^iPr)_{20}$, $a = 16.996(6)$ Å, $b = 10.014(3)$ Å, $c = 24.924(9)$ Å, and $\beta = 105.86(1)°$ with $Z = 2$.

Introduction

We are interested in developing systematic principles for the synthesis of heterometallic alkoxides which might serve as precursors (via hydrolysis or chemical vapor deposition) to ternary oxides $M_aM'_bO_p$. We have reported how the change from isopropoxide to *tert*-butoxide alters the K:Zr stoichiometry from $KZr_2(O^iPr)_9$ to $KZr_2(O^tBu)_9$ *and* $[KZr(O^tBu)_5]_2$,[1] and thus a larger alkoxide substituent leads to a lower accessible coordination number for zirconium in the last of these three compounds.

We continue to report here on the effect of R group size in an alkoxide OR, together with a study of the influence of the size of *each* metal in heterometallic tin and lead alkoxides containing either titanium or zirconium. In addition to stoichiometry ($M^{II}_aM^{IV}_b(OR)_{2a+4b}$), we wish to establish the effect of these molecular parameters on degree of aggregation and on solubility, volatility, and thermal decomposition behavior.

Relevant earlier syntheses of compounds in this class include salt metathesis[2] (eq 1) and direct adduct formation[3] (eq 2) of the *in situ*-formed $Pb(O^tBu)_2$ with $Zr(O^tBu)_4$.

$$Tl_2Zr(OEt)_6 + PbI_2 \rightarrow \text{“}PbZr(OEt)_6\text{”} + 2TlI \qquad (1)$$

$$Pb[N(SiMe_3)_2]_2 + Zr(O^tBu)_4 + 2{}^tBuOH \rightarrow PbZr(O^tBu)_6 + 2HN(SiMe_3)_2 \qquad (2)$$

Experimental Section

All manipulations were carried out under an atmosphere of dry nitrogen or argon using standard Schlenk techniques. All solvents and alcohols were dried appropriately, distilled prior to use, and stored over molecular sieves under dry nitrogen. $Zr_2(O^iPr)_8(HO^iPr)_2$ was purchased from Aldrich and recrystallized from HO^iPr/pentane; all HO^iPr can be removed from the solid alcohol adduct under dynamic vacuum (1 h at 100 °C) to leave $Zr(O^iPr)_4$.[4] $Zr(O^tBu)_4$ was prepared according to a modification of the literature procedure[5] using $Zr(NMe_2)_4$.[6] Coordinated amine was removed by distillation of the product under dynamic vacuum (80 °C, 10^{-2} Torr). $M[N(SiMe_3)_2]_2$ (M = Sn, Pb)[7] and $[M(O^tBu)_2]_n$ (M = Sn,[8] Pb[9]) were prepared according to literature procedures.[9] $[Pb(O^iPr)_2]_n$ was prepared according to a modification of a literature procedure. Synthesis at −40 °C in pentane afforded a white, flocculant precipitate, which was washed three times with pentane and dried 12 h under dynamic vacuum (10^{-2} Torr). ^1H and ^{13}C NMR spectra were recorded on a Varian XL 300 or Bruker AM 500 spectrometer, and chemical shifts were referenced to the protio impurity or ^{13}C signal of the solvent, respectively. ^{119}Sn and ^{207}Pb NMR spectra were recorded on a Bruker AM 500 spectrometer with chemical shifts referenced to external standards (^{119}Sn: $SnMe_4$, 17% in toluene, 0.0 ppm. ^{207}Pb: $PbEt_4$, neat, 73.3 ppm[10]), with positive shifts being to higher frequencies. Elemental analyses were performed by Desert Analytics.

Synthesis of $SnZr(O^tBu)_6$. $[Sn(O^tBu)_2]_2$ (1.06 g, 2.00 mmol) was dissolved in 20 mL of ether, and the solution was slowly added to $Zr(O^tBu)_4$ (1.54 g, 4.01 mmol) in 20 mL of ether. The resulting solution was stirred for 10 min at 25 °C, concentrated to ~15 mL, and placed in a freezer. Crystallization at −20 °C produced 2.17 g (83.5%) of colorless, hexagonal pillars. Sublimation of this product occurs at 120 °C (10^{-2} Torr). ^1H NMR (C_6D_6, 25 °C): δ 1.54 (s, 27H), 1.46 (s, 27H). $^{13}C\{^1H\}$ NMR (C_6D_6, 25 °C): δ 75.5 (s, $\mathit{C}(CH_3)_3$), 73.4 (s, $\mathit{C}(CH_3)_3$), 34.2 (s, $C(\mathit{C}H_3)_3$, $^3J_{^{117,119}Sn-^{13}C} = 28.1$ Hz), 33.6 (s, $C(\mathit{C}H_3)_3$). ^{119}Sn NMR (toluene-d_8, 25 °C): δ −234. Anal. Calcd for $SnZrO_6C_{24}H_{54}$: C, 44.44; H, 8.39. Found: C, 43.37; H, 8.24.

Synthesis of $PbZr(O^tBu)_6$. $[Pb(O^tBu)_2]_3$ (0.75 g, 0.71 mmol) and $Zr(O^tBu)_4$ (0.82 g, 2.14 mmol) were placed together in a flask and dissolved in 40 mL of ether, and the mixture was stirred for 30 min. The solution was concentrated to ~20 mL and placed in a −20 °C freezer. This crystallization gave 0.682 g (43.4%) of colorless, hexagonal pillars (yield not optimized). Sublimation of this product occurs at 120 °C (10^{-2} Torr). ^1H NMR (C_6D_6, 25 °C): δ 1.59 (s, 27H), 1.41 (s, 27H). $^{13}C\{^1H\}$ NMR (C_6D_6, 25 °C): δ 75.0 (s, $\mathit{C}(CH_3)_3$), 72.3 (s, $\mathit{C}(CH_3)_3$), 35.1 (s, $C(\mathit{C}H_3)_3$, $^3J_{^{207}Pb-^{13}C} = 29.0$ Hz), 33.8 (s, $C(\mathit{C}H_3)_3$). ^{207}Pb NMR (toluene-d_8, 25 °C): δ 1394. Anal. Calcd for $PbZrO_6C_{24}H_{54}$: C, 39.10; H, 7.40. Found: C, 38.76; H, 7.40.

[⊗] Abstract published in *Advance ACS Abstracts,* April 15, 1996.

(1) Teff, D. J.; Huffman, J. C.; Caulton, K. G. *Inorg. Chem.* **1994**, *33*, 6289.

(2) Hampden-Smith, M. J.; Wark, T. A.; Jones, L. C.; Brinker, C. J. *Ceram. Trans.* **1992**, *25*, 187.

(3) Vaartstra, B. A. *Mater. Res. Soc. Symp. Proc.* **1993**, *282*, 689.

(4) Xue, Z.; Vaartstra, B. A.; Caulton, K. G.; Chisholm, M. H.; Jones, D. L. *Eur. J. Solid State Inorg. Chem.* **1992**, *29*, 213.

(5) Thomas, I. M. *Can. J. Chem.* **1961**, *39*, 1386.

(6) Chisholm, M. H.; Hammond, C. E.; Huffman, J. C. *Polyhedron* **1988**, *7*, 2515.

(7) Harris, D. H.; Lappert, M. F. *J. Chem. Soc., Chem. Commun.* **1974**, 895.

(8) (a) Fjeldberg, T.; Hitchcock, P. B.; Lappert, M. F.; Smith, S. J.; Thorne, A. J. *J. Chem. Soc., Chem. Commun.* **1985**, 939. (b) Veith, H.; Hobein, P.; Rösler, R. *Z. Naturforsch.* **1989**, *44B*, 1067.

(9) Goel, S. C.; Chiang, M. Y.; Buhro, W. E. *Inorg. Chem.* **1990**, *29*, 4640.

(10) Kennedy, J. D.; McFarlane, W.; Pyne, G. S. *J. Chem. Soc., Dalton Trans.* **1977**, 2332.

S0020-1669(95)01413-3 CCC: $12.00

Synthesis of SnZr(O^{i}Pr)$_6$. Sn[N(SiMe$_3$)$_2$]$_2$ (3.11 g, 7.08 mmol) was dissolved in 40 mL of pentane, and the solution was cooled to −30 °C, after which it was cannula-transferred dropwise to Zr$_2$(O^{i}Pr)$_8$(HO-^{i}Pr)$_2$ (2.75 g, 3.55 mmol) in 50 mL of pentane at −30 °C. Upon addition of 0.55 mL of neat HO^{i}Pr (7.19 mmol), the light yellow solution became colorless. The reaction mixture was warmed to 25 °C, and the solvent was then removed *in vacuo*, producing an oil. Further removal of the solvent was encouraged at 40 °C, and solid began to sublime after 1 h. The entire solid was transferred to a sublimation apparatus, where 3.27 g (81.9%) of waxy solid sublimed as a crystalline mass at 55 °C (10^{-2} Torr). ^{1}H NMR (C$_6$D$_6$): δ 4.61 (septet, 3H, $^3J_{\mathrm{H-H}} = 6$ Hz), 4.54 (septet, 3H, $^3J_{\mathrm{H-H}} = 6$ Hz), 1.39 (d, 18H, $^3J_{\mathrm{H-H}} = 6$ Hz), 1.29 (d, 18H, $^3J_{\mathrm{H-H}} = 6$ Hz). ^{13}C{^{1}H} NMR (C$_6$D$_6$, 25 °C): δ 70.7 (s, *C*H(CH$_3$)$_2$), 68.5 (s, *C*H(CH$_3$)$_2$), 27.9 (s, CH(*C*H$_3$)$_2$), 27.6 (s, CH(*C*H$_3$)$_2$). ^{119}Sn NMR (toluene-*d*$_8$, 25 °C): δ −260. Anal. Calcd for SnZrO$_6$C$_{18}$H$_{42}$: C, 38.30; H, 7.50. Found: C, 38.18; H, 7.41.

Synthesis of Pb$_4$Zr$_2$(O^{i}Pr)$_{16}$ and Pb$_2$Zr$_4$(O^{i}Pr)$_{20}$. Pb[N(SiMe$_3$)$_2$]$_2$ (3.41 g, 6.46 mmol) dissolved in 30 mL of ether was added dropwise to Zr$_2$(O^{i}Pr)$_8$(HO^{i}Pr)$_2$ (2.50 g, 3.22 mmol) in 40 mL of −40 °C ether. After complete addition, neat HO^{i}Pr (0.50 mL, 6.54 mmol) was added dropwise to the turbid, yellow solution. This gave a white precipitate suspended in a colorless solution. This precipitate began to disappear upon warming of the solution to 25 °C, and a clear solution remained after stirring for 20 min at 25 °C. Multiple recrystallizations from ether (−20 °C) produced colorless crystals of Pb$_2$Zr$_4$(O^{i}Pr)$_{20}$ (0.32 g, 15%).[11] ^{1}H NMR (C$_6$D$_6$, 25 °C): δ 4.69 (br septet, $^3J_{\mathrm{H-H}} = 6$ Hz), 1.45 (d, $^3J_{\mathrm{H-H}} = 6$ Hz). ^{13}C{^{1}H} NMR (C$_6$D$_6$, 25 °C): δ 71.0 (s, *C*H(CH$_3$)$_2$), 27.0 (s, CH(*C*H$_3$)$_2$). Multiple recrystallizations of the remaining material from toluene (−20 °C) produced colorless crystals of Pb$_4$Zr$_2$(O^{i}Pr)$_{16}$ (1.61 g, 76.5%).[11] ^{1}H NMR (C$_6$D$_6$, 25 °C): δ 5.03 (br), 1.41 (d, $^3J_{\mathrm{H-H}} = 5$ Hz).

Synthesis of Pb$_4$Zr$_2$(O^{i}Pr)$_{16}$. Pb[N(SiMe$_3$)$_2$]$_2$ (0.809 g, 1.53 mmol) was dissolved in 40 mL of ether, and the solution was taken to −40 °C, whereupon neat HO^{i}Pr (234 μL, 3.06 mmol) was added. This resulted in formation of a white, flocculant precipitate suspended in a clear, colorless solution. The reaction mixture was warmed to room temperature and stirred for 10 min. The solvent was subsequently removed *in vacuo*, and the solid was dried at 40 °C under dynamic vacuum for 30 min. The solid was suspended in 50 mL of toluene, and Zr(O^{i}Pr)$_4$ (0.251 g, 0.767 mmol) dissolved in 10 mL of toluene was added dropwise. This decreased the amount of white solid present. After the reaction mixture was stirred for 30 min at 90 °C, the solution was filtered through Celite, reduced to ~25 mL, and placed in a −20 °C freezer; 0.32 g (43%) of solid was isolated. ^{1}H NMR (C$_6$D$_6$, 25 °C): δ 4.98 (br, 16H), 1.40 (d, 96H, $^3J_{\mathrm{H-H}} = 6$ Hz). ^{1}H NMR data (toluene-*d*$_8$) are as follows. 25 °C: δ 5.02 (br, 16H), 1.39 (d, 96H, $^3J_{\mathrm{H-H}} = 6$ Hz). 0 °C: δ 5.85 (br, 4H), 4.89 (br, 12H), 1.41 (d, 96H, $^3J_{\mathrm{H-H}} = 6$ Hz). −30 °C: δ 6.04 (vbr, 4H), 5.16 (br, 6H), 4.64 (br, 6H), 1.45 (br, 96H). −60 °C: δ 6.50 (br, 2H), 5.78 (br, 2H), 5.32 (br, 2H), 4.85 (br septet, 4H, $^3J_{\mathrm{H-H}} = 6$ Hz), 4.69 (br septet, 6H, $^3J_{\mathrm{H-H}} = 6$ Hz), 1.55−1.43 (br, 96H). ^{13}C{^{1}H} NMR (C$_6$D$_6$, 25 °C): δ 68.5 (s, *C*H(CH$_3$)$_2$), 28.5 (s, CH(*C*H$_3$)$_2$). ^{207}Pb NMR (toluene-*d*$_8$, −20 °C): δ 950 (s, 2Pb), 804 (s, 2Pb). Anal. Calcd for Pb$_4$Zr$_2$O$_{16}$C$_{48}$H$_{112}$: C, 29.47; H, 5.77. Found: C, 29.02; H, 5.74.

Synthesis of Pb$_2$Zr$_4$(O^{i}Pr)$_{20}$. Pb[N(SiMe$_3$)$_2$]$_2$ (2.69 g, 5.09 mmol) dissolved in 30 mL of pentane was added dropwise to Zr$_2$(O^{i}Pr)$_8$(HO-^{i}Pr)$_2$ (3.95 g, 5.09 mmol) in 30 mL of pentane at −40 °C. After the first few drops were added, a white precipitate formed. Following complete addition of the amide, the reaction mixture was warmed to room temperature, giving a clear, colorless solution. This solution was stirred for 30 min at 25 °C and concentrated to ~35 mL. Crystallization at −20 °C gave 3.76 g (75%) of crystalline solid. ^{1}H NMR (C$_6$D$_6$, 25 °C): δ 4.68 (br septet, 20H, $^3J_{\mathrm{H-H}} = 6$ Hz), 1.45 (d, 120H, $^3J_{\mathrm{H-H}} = 6$ Hz). ^{1}H NMR data (toluene-*d*$_8$) are as follows. 25 °C: δ 4.67 (br septet, 20H, $^3J_{\mathrm{H-H}} = 6$ Hz), 1.44 (d, 120 Hz, $^3J_{\mathrm{H-H}} = 6$ Hz). −30 °C: δ 5.95 (vbr, 2H), 4.62 (br, 18H), 1.48 (br, 120H). −40 °C: δ 6.14 (br, 2H), 4.91 (br, 4H), 4.58 (br, 14H), 1.71 (br, 12H), 1.47 (br, 108H). −60 °C: δ 6.21 (br, 2H), 4.94 (br, 4H), 4.73 (br septet, 2H, $^3J_{\mathrm{H-H}} =$ 6 Hz), 4.58 (br septet, 12H, $^3J_{\mathrm{H-H}} = 6$ Hz), 1.74−1.47 (br, 120H). ^{13}C{^{1}H} NMR (C$_6$D$_6$, 25 °C): δ 71.0 (s, *C*H(CH$_3$)$_2$), 27.1 (s, CH(*C*H$_3$)$_2$). ^{207}Pb NMR (toluene-*d*$_8$, 65 °C): δ 1002. Anal. Calcd for Pb$_2$Zr$_4$O$_{20}$C$_{60}$H$_{140}$: C, 36.75; H, 7.20. Found: C, 36.13; H, 7.48.

Table 1. Crystallographic Data for Pb$_4$Zr$_2$(O^{i}Pr)$_{16}$ (**1**) and Pb$_2$Zr$_4$(O^{i}Pr)$_{20}$ (**2**)

	1	**2**
formula	C$_{48}$H$_{112}$O$_{16}$Pb$_4$Zr$_2$	C$_{60}$H$_{140}$O$_{20}$Pb$_2$Zr$_4$
a, Å	12.190(6)	16.996(6)
b, Å	14.701(7)	10.014(3)
c, Å	19.978(13)	24.924(9)
β, deg	105.57(3)	105.86(1)
V, Å^3	3448.85	4080.41
Z	2	2
fw	1956.64	1961.03
space group	$P2_1/c$	$P2_1/c$
T, °C	−174	−174
λ, Å	0.710 69	0.710 69
ϱ_{calcd}, g cm^{-3}	1.884	1.596
μ(Mo Kα), cm^{-1}	101.5	46.9
R^a	0.0647	0.0913
$R_w{}^b$	0.0636	0.0812

^{a} $R = \sum||F_o| - |F_c||/\sum|F_o|$. ^{b} $R_w = [\sum w(|F_o| - |F_c|)^2/\sum w|F_o|^2]^{1/2}$ where $w = 1/\sigma^2(|F_o|)$.

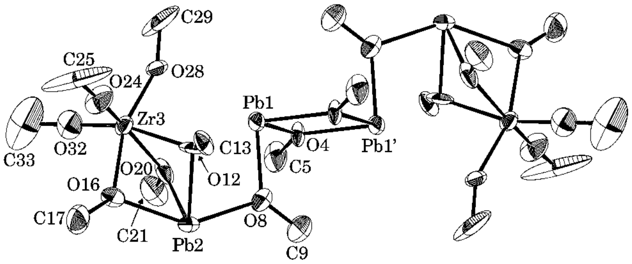

Figure 1. ORTEP drawing of Pb$_4$Zr$_2$(O^{i}Pr)$_{16}$, with methyl groups omitted for clarity. Unlabeled atoms are related to those shown by a crystallographic center of symmetry between Pb1 and Pb1′.

Structure Determination of Pb$_4$Zr$_2$(O^{i}Pr)$_{16}$. A small, well-formed crystal was cleaved from a larger sample and affixed to the end of a glass fiber using silicone grease; the mounted sample was then transferred to a goniostat where it was cooled to −174 °C for characterization and data collection (6° < 2θ < 45°). Standard inert-atmosphere handling techniques were used throughout the investigation. A systematic search of a limited hemisphere of reciprocal space located a set of data with monoclinic symmetry and systematic absences corresponding to the unique space group $P2_1/c$. Subsequent solution and refinement of the structure confirmed this to be the proper space group. Data were collected (Table 1) using a standard moving-crystal, moving-detector technique with fixed background counts at each extreme of the scan. The crystal was lost because of icing problems with the cold stream, which prevented an accurate absorption correction. Data were corrected for Lorentz and polarization terms and equivalent data averaged. The structure was solved by direct methods (MULTAN 78) and Fourier techniques. Hydrogen atoms were introduced into fixed, idealized positions. No atttempt was made to include hydrogen atoms in the refinement. A final difference Fourier map was essentially featureless, although there were several peaks of intensity 1.0−2.0 e/Å^3 at the lead atom positions. The results are shown in Table 2 and Figures 1 and 3.

Structure Determination of Pb$_2$Zr$_4$(O^{i}Pr)$_{20}$. A small fragment was cleaved from a twinned crystal and affixed to the end of a glass fiber using silicone grease; the mounted sample was then transferred to the goniostat where it was cooled to −174 °C for characterization and data collection. Eight different samples were examined before one was found that was not severely twinned. Standard inert-atmosphere handling techniques were used throughout the investigation. A systematic search of a limited hemisphere of reciprocal space located a set of reflections with monoclinic symmetry (Table 1) and systematic absences corresponding to the unique space group $P2_1/c$. Subsequent solution and refinement of the structure confirmed this to be the proper

---

(11) Yield calculations based on synthesis of Pb$_2$Zr$_4$(O^{i}Pr)$_{20}$ and Pb$_4$Zr$_2$(O-^{i}Pr)$_{16}$ in a 1:1 ratio.

Table 2. Selected Bond Distances (Å) and Angles (deg) for $Pb_4Zr_2(O^iPr)_{16}$

(a) Distances			
Pb1−O4	2.303(15)	Zr3−O12	2.271(21)
Pb1−O4′	2.336(17)	Zr(3)−O(16)	2.135(17)
Pb1−O8	2.241(20)	Zr3−O20	2.256(19)
Pb2−O8	2.431(20)	Zr3−O24	1.931(23)
Pb2−O12	2.293(17)	Zr3−O28	1.995(18)
Pb2−O16	2.392(19)	Zr3−O32	1.855(23)
Pb2−O20	2.232(21)		
(b) Angles			
O4−Pb1−O4′	72.1(6)	O24−Zr3−O28	100.4(9)
O4−Pb1−O8	89.6(7)	O24−Zr3−O32	97.7(10)
O4′−Pb1−O8	90.2(7)	O28−Zr3−O32	101.2(8)
O8−Pb2−O12	81.7(7)	Pb1−O4−Pb1′	107.9(6)
O8−Pb2−O16	143.8(6)	Pb1−O4−C5	130.8(16)
O8−Pb2−O20	78.4(7)	Pb1−O4′−C5′	118.5(16)
O12−Pb2−O16	70.0(7)	Pb1−O8−Pb2	107.5(8)
O12−Pb2−O20	69.9(7)	Pb1−O8−C9	126.1(21)
O16−Pb2−O20	71.0(6)	Pb2−O8−C9	126.4(21)
O12−Zr3−O16	75.1(7)	Pb2−O12−Zr3	93.7(7)
O12−Zr3−O20	69.8(7)	Pb2−O12−C13	118.0(16)
O12−Zr3−O24	95.0(9)	Zr3−O12−C13	124.1(17)
O12−Zr3−O28	87.6(7)	Pb2−O16−Zr3	94.5(6)
O12−Zr3−O32	163.0(9)	Pb2−O16−C17	131.1(19)
O16−Zr3−O20	75.5(8)	Zr3−O16−C17	134.2(20)
O16−Zr3−O24	91.5(9)	Pb2−O20−Zr3	95.8(8)
O16−Zr3−O28	159.8(7)	Pb2−O20−C21	115.6(18)
O16−Zr3−O32	93.2(8)	Zr3−O20−C21	133.9(19)
O20−Zr3−O24	161.9(9)	Zr3−O24−C25	172(4)
O20−Zr3−O28	89.0(7)	Zr3−O28−C29	151.6(23)
O20−Zr3−O32	95.5(9)	Zr3−O32−C33	169.5(27)

Table 3. Bond Distances (Å) and Angles (deg) for $Pb_2Zr_4(O^iPr)_{20}$

(a) Distances			
Pb1−O4	2.239(22)	Zr2−O28	2.225(21)
Pb1−O4′	2.425(21)	Zr3−O20	2.190(21)
Pb1−O8	2.309(21)	Zr3−O24	2.261(22)
Zr2−O8	2.168(21)	Zr3−O28	2.269(22)
Zr2−O12	1.926(22)	Zr3−O32	1.973(21)
Zr2−O16	1.932(22)	Zr3−O36	1.939(22)
Zr2−O20	2.267(21)	Zr3−O40	1.886(24)
Zr2−O24	2.158(23)		
(b) Angles			
O4−Pb1−O4′	71.5(9)	O24−Zr3−O40	95.8(9)
O4−Pb1−O8	86.0(8)	O28−Zr3−O32	89.8(8)
O4′−Pb1−O8	96.2(7)	O28−Zr3−O36	96.5(8)
O4−Pb1−O28	167.3(9)	O28−Zr3−O40	159.8(9)
O8−Zr2−O12	98.9(9)	O32−Zr3−O36	99.5(9)
O8−Zr2−O16	97.8(9)	O32−Zr3−O40	100.3(9)
O8−Zr2−O20	78.9(8)	O36−Zr3−O40	98.9(10)
O8−Zr2−O24	149.1(8)	Pb1−O4−Pb1′	108.5(9)
O8−Zr2−O28	84.5(8)	Pb1−O4−C5	124.7(19)
O12−Zr2−O16	99.0(9)	Pb1−O4′−C5′	119.2(19)
O12−Zr2−O20	163.4(8)	Pb1−O8−Zr2	106.3(9)
O12−Zr2−O24	103.7(9)	Pb1−O8−C9	118.5(17)
O12−Zr2−O28	95.0(9)	Zr2−O8−C9	135.1(18)
O16−Zr2−O20	97.6(8)	Zr2−O12−C13	167.0(23)
O16−Zr2−O24	99.1(9)	Zr2−O16−C17	164.3(22)
O16−Zr2−O28	165.3(9)	Zr2−O20−Zr3	95.5(8)
O20−Zr2−O24	73.3(8)	Zr2−O20−C21	125.2(17)
O20−Zr2−O28	68.4(8)	Zr3−O20−C21	129.7(18)
O24−Zr2−O28	72.9(8)	Zr2−O24−Zr3	96.6(9)
O20−Zr3−O24	72.9(8)	Zr2−O24−C25	130.7(17)
O20−Zr3−O28	69.0(8)	Zr3−O24−C25	132.0(17)
O20−Zr3−O32	90.1(8)	Zr2−O28−Zr3	94.5(8)
O20−Zr3−O36	162.7(9)	Zr2−O28−C29	125.9(20)
O20−Zr3−O40	93.4(9)	Zr3−O28−C29	123.4(19)
O24−Zr3−O28	70.2(8)	Zr3−O32−C33	162.7(20)
O24−Zr3−O32	157.2(8)	Zr3−O36−C37	171.5(22)
O24−Zr3−O36	93.7(8)	Zr3−O40−C41	158.7(25)

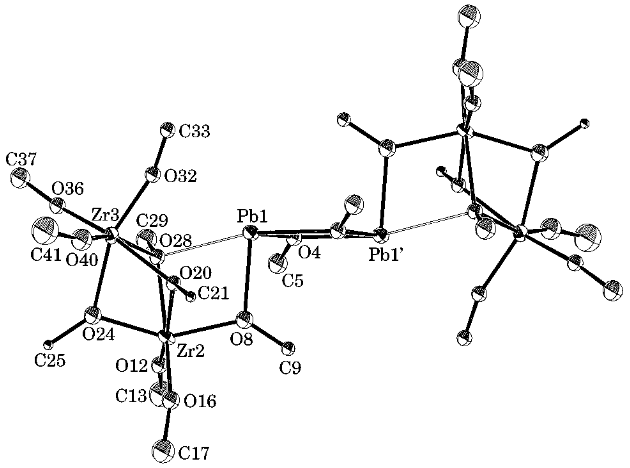

Figure 2. ORTEP drawing of $Pb_2Zr_4(O^iPr)_{20}$, with methyl groups omitted for clarity. Unlabeled atoms are related to those shown by a crystallographic center of symmetry between Pb1 and Pb1′. The "open" bond shows a weak interaction between O28 and Pb1.

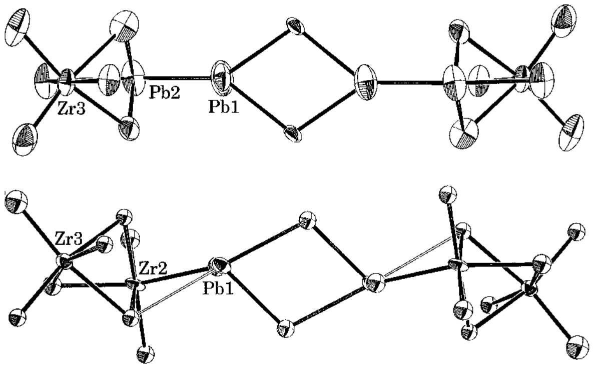

Figure 3. Drawings of the inner coordination spheres of $Pb_4Zr_2(O{}^iPr)_{16}$ (upper) and $Pb_2Zr_4(O^iPr)_{20}$ (lower) viewed down the Pb1−O8 bond. This shows the modest nonplanarity of the six metals in the latter case, as well as the lengthening of the Pb1−O4 bonds (2.43(2) *vs* 2.24(2) Å for Pb1−O4′) as a result of the open bond (2.72 Å) drawn to Pb1.

space group. Data were collected (6° < 2θ < 45°) using a standard moving-crystal, moving-detector technique with fixed background counts at each extreme of the scan. Data were corrected for Lorentz and polarization terms and equivalent data averaged after correction for absorption. The structure was solved by direct methods (SHELXTL-PC) and Fourier techniques. A difference Fourier map phased on the non-hydrogen atoms located three large peaks which did not make chemical sense. Examination of the location of these peaks indicated that they were undoubtedly due to the *ca.* 10% twin fragment present. When they were included as partial-occupancy Zr atoms, the residual dropped from 0.13 to 0.09. The "occupancy" of the three atoms [M(A), M(B), and M(C)] converged to values 9.9%, 8.2%, and 10.6%. No attempt was made to refine any atoms of the twin fragment except the three unique metals. Hydrogen atoms were included as fixed atom contributors. A final difference Fourier map contained numerous peaks with intensities up to 2.1 e/Å^3. The results are shown in Table 3 and Figures 2 and 3.

Results

O^{t}Bu as a Ligand. In a slight variation of the reported study,[3] we find that $Zr(O^tBu)_4$, a four-coordinate monomer (by mass spectrometry[4] and solution molecular weight measurements[12]), reacts with the trimer[9] $[Pb(O^tBu)_2]_3$, of structure $Pb(\mu\text{-}O^tBu)_3Pb(\mu\text{-}O^tBu)_3Pb$, to produce $PbZr(O^tBu)_6$. This is a colorless, crystalline solid which is soluble in aliphatic and aromatic hydrocarbons and sublimes unchanged (^1H NMR evidence) at 120 °C and 10^{-2} Torr. It exhibits two alkoxide environments (of equal intensity) by both ^1H and ^{13}C NMR

---

(12) Bradley, D. C.; Mehrotra, R. C.; Wardlaw, W. *J. Chem. Soc.* **1952**, 4204.

spectroscopy in benzene at 25 °C. Although any coupling to ^{207}Pb is too small to be resolved at the quaternary carbons, *one* of the two types of methyl carbons shows 29 Hz doublet satellites due to $^3J_{^{207}\mathrm{Pb-C}}$. A single environment is seen by ^{207}Pb NMR spectroscopy at 25 °C in toluene. The mass spectrum shows a number of fragments ($400 < m/e < 700$), one of which indicates loss of $\mathrm{O^tBu^-}$ ($m/e = 663$ for $\mathrm{PbZr(O^tBu)_5^+}$). This suggests a monomeric structure with only half of the alkoxides directly bonded to lead (**I**). This incorporates the common

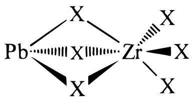

X = O^{t}Bu

I

coordination numbers of 3 and 6, respectively, for Pb and Zr. Although numerous crystals, formed both from solution ($\mathrm{Et_2O}$, −20 °C) and by sublimation, have been examined by single-crystal X-ray diffraction, full data sets could not be solved, apparently due to 180° disorder of the Pb/Zr vector.

In contrast to the case of $\mathrm{[Pb(O^tBu)_2]_3}$, tin forms a *dimeric* O^{t}Bu compound,[8] symptomatic of its smaller size. Nevertheless, $\mathrm{SnZr(O^tBu)_6}$, the Sn analog of $\mathrm{PbZr(O^tBu)_6}$, is formed when $\mathrm{[Sn(O^tBu)_2]_2}$ reacts with $\mathrm{Zr(O^tBu)_4}$ in a 1:1 Sn:Zr ratio. This molecule sublimes intact at 120 °C and 10^{-2} Torr and, as for $\mathrm{PbZr(O^tBu)_6}$, is believed to be a monomer in the gas phase from its mass spectrum, which shows a fragment consistent with the loss of $\mathrm{O^tBu^-}$ ($m/e = 575$ for $\mathrm{SnZr(O^tBu)_5^+}$). $\mathrm{SnZr(O^tBu)_6}$ exhibits two equal-intensity peaks for the ^{1}H, quaternary carbon, and methyl carbon regions of its NMR spectra. Again, only one of the two types of methyl carbons is found to couple to a spin-active metal (^{117}Sn and ^{119}Sn), resulting in 28 Hz doublet satellites. A single resonance at −234 ppm is seen in its ^{119}Sn NMR spectrum (toluene, 25 °C). All evidence thus indicates that tin and lead are able to form isostructural and molecular *tert*-butoxide compounds. X-ray diffraction data sets collected on crystals grown from hot toluene (cooled to 25 °C) were similar to those of $\mathrm{PbZr(O^tBu)_6}$ and thus could not be solved.

O^{i}Pr as a Ligand. An attempted synthesis of an analogous 1:1 Pb:Zr compound for isopropoxide in fact takes a very different course. Reaction according to eq 3 in $\mathrm{Et_2O}$ at −40

$$\mathrm{3Zr_2(O^iPr)_8(^iPrOH)_2 + 6Pb[N(SiMe_3)_2]_2 + 6\,^iPrOH \rightarrow Pb_2Zr_4(O^iPr)_{20} + Pb_4Zr_2(O^iPr)_{16} + 12HN(SiMe_3)_2} \quad (3)$$

°C, followed by concentration of the ether solvent to incipient crystallization and cooling, gives a colorless crystalline solid which shows only one isopropoxide environment (^{1}H, ^{13}C NMR) at 25 °C. Solubility differences and multiple recrystallizations can be used to isolate the second Pb/Zr product.

A single product is formed from the reaction of polymeric $\mathrm{[Pb(O^iPr)_2]}_n$ with $\mathrm{Zr(O^iPr)_4}$ in the correct stoichiometry (eq 4).

$$(4/n)\mathrm{[Pb(O^iPr)_2]}_n + \mathrm{2Zr(O^iPr)_4} \xrightarrow{\Delta} \mathrm{Pb_4Zr_2(O^iPr)_{16}} \quad (4)$$

In contrast to those used for the synthesis of $\mathrm{PbZr(O^tBu)_6}$, the reactants must be heated to 80 °C for a few minutes[13] to depolymerize $\mathrm{[Pb(O^iPr)_2]}_n$. This method gives a single product (NMR evidence).

Attempted sublimation of this high molecular weight species at 120 °C and 10^{-2} Torr results in decomposition to a colorless solid of unknown composition. ^{1}H NMR spectroscopy of the sublimate shows a number of sharp peaks in both the methine and methyl regions which do not correspond to known compounds.

Solid-State Structure. The solid-state structure of $\mathrm{Pb_4Zr_2(O^iPr)_{16}}$ is rigorously centrosymmetric (Figure 1), but there is also an idealized mirror plane of symmetry for the $\mathrm{Pb_4Zr_2O_{16}}$ core containing Pb1, Pb2, and Zr3 (upper half of Figure 3). That is, all six metals lie on the idealized mirror plane. The structure contains two $\mathrm{(^iPrO)_3Zr(\mu\text{-}O^iPr)_3Pb}$ units analogous to **I** (isolated above for O^{t}Bu), but they are linked by a $\mathrm{Pb_2(O^iPr)_4}$ unit. The latter has a $\mathrm{Pb_2(O^iPr)_2(\mu\text{-}O^iPr)_2}$ structure, analogous to that of $\mathrm{[Sn(O^tBu)_2]_2}$,[8] and each of the "terminal" O^{i}Pr units of such a dimer donate additionally to one Pb2 of the $\mathrm{PbZr(O^iPr)_6}$ units. Thus, Pb1 is three-coordinate and Pb2 is four-coordinate while zirconium is six-coordinate (structure **A**, X = O^{i}Pr). The driving force for this higher (than $\mathrm{PbZr(OR)_6}$) degree of aggregation is thus the higher coordination number at the larger Pb made possible by the smaller O^{i}Pr group.

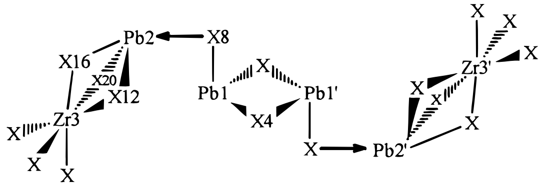

A

The coordination geometry of Pb1 is highly pyramidal (O−Pb−O angles 72.1(6)−90.2(7)°), whereas the geometry of Pb2 is pseudo trigonal bipyramidal, with O8 and O16 axial (∠O8−Pb2−O16 = 143.8(6)°) and O12 and O20 equatorial. The remaining equatorial position is vacant. The linkage O8−Pb2 is the weakest in the molecule (2.43(2) Å), in comparison to the short Pb1−O8 (2.24(2) Å) and the Pb1−O4 (2.30(2) and 2.34(2) Å) distances. The Pb2−O distances to alkoxides also bound to Zr are 2.23(2)−2.39(2) Å. Oxygens O4, O8, and O16 are essentially coplanar with their attached substituents (angles sum to 357.2−360.0°), while O12 and O20 are distinctly pyramidal (angles sum to 335.8−345.3°). This correlates strongly with the fact that the Zr3−O16 distance (2.14(2) Å) is distinctly shorter than the Zr3−O12 (2.27(2) Å) and −O20 (2.26(2) Å) distances. Indeed, O16 is most asymmetrically placed, having the longest Pb2−O distance (2.39(2) Å) of these bridging groups. The Ot−Zr−Ot angles (97.7(10)−101.2(8)°) are larger than the Ot−Zr−μO angles (87.6(7)−95.5(9)°), which are in turn larger than the μO′−Zr−μO angles (69.8(7)−75.5(8)°). While the Zr−O−C angles at two of the terminal O^{i}Pr ligands are nearly linear (170(3) and 172(4)°), that at O28 is quite bent (152(3)°), apparently due to repulsion between the ^{i}Pr group and Pb1. The nonplanarity at O12 and O20 may have the same cause.

The $\mathrm{Pb_2Zr(O^iPr)_8}$ unit (i.e., half the $\mathrm{Pb_4Zr_2(O^iPr)_{16}}$ dimer) shown in **II** is related to the general structure $\mathrm{M_3X_5}$ (**III**) which is often seen in $\mathrm{M_3}$ alkoxide chemistry.[14] However, **II** lacks the bonds a, b, and c seen in the $\mathrm{M_3X_5}$ unit. Thus, the

---

(13) Note that decomposition of lead alkoxides to oxo alkoxides has been observed upon heating for extended periods of time: Papiernik, R.; Hubert-Pfalzgraf, L. G.; Chaput, F. *J. Non-Cryst. Solids* **1992**, *147*, 36.

(14) (a) $\mathrm{[Mo_3O(O^iPr)_{10}]}$: Chisholm, M. H.; Folting, K.; Huffman, J. C.; Kirkpatrick, C. C. *Inorg. Chem.* **1984**, *23*, 1021. (b) $\mathrm{[U_3O(OCMe_3)_{10}]}$: Cotton, F. A.; Marler, D. O.; Schwotzer, W. *Inorg. Chim. Acta* **1984**, *95*, 207. (c) $\mathrm{[W_3O(O^iPr)_{10}]}$: Chisholm, M. H.; Folting, K.; Huffman, J. C.; Kober, E. M. *Inorg. Chem.* **1985**, *24*, 241. (d) $\mathrm{[BaZr_2(O^iPr)_{10}]_2}$: Vaartstra, B. A.; Huffman, J. C.; Streib, W. E.; Caulton, K. G. *Inorg. Chem.* **1991**, *30*, 3068. (e) $\mathrm{[ClCuZr_2(O^iPr)_9]}$: Vaartstra, B. A.; Samuels, J. A.; Barash, E. H.; Martin, J. D.; Streib, W. E.; Gasser, C.; Caulton, K. G. *J. Organomet. Chem.* **1993**, *449*, 191. (f) $\mathrm{[YBa_2(O^tBu)_7(HO^tBu)]}$: Borup, B.; Streib, W. E.; Caulton, K. G. *Inorg. Chem.*, submitted for publication.

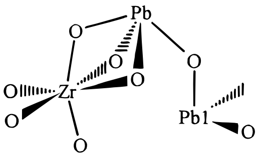

II

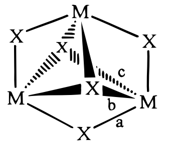

III

coordination number at Pb1 is 3. Such closure of the six-membered ring would give Pb(II) an unusually high coordination number of 6.

In spite of the long O8−Pb2 linkage, $\mathrm{Pb_4Zr_2(O^iPr)_{16}}$ appears to stay intact in aromatic solvents. The methine region is particularly informative since large differences in chemical shifts are seen in the decoalesced (−60 °C) methine region (6.50−4.69 ppm) as compared to the methyl region (1.55−1.43 ppm). Also, in the presence of prochiral centers (Pb2, Zr3), methyl groups on $\mathrm{O^iPr}$ ligands not on the plane containing all metals become diastereotopic. The ^{1}H NMR of the methine hydrogens at −60 °C in toluene-d_8 (300 MHz) shows five multiplets of relative intensity 2:2:2:4:6. These we assign to $\mathrm{(Pb1)_2(\mu\text{-}O^iPr)_2}$, $\mathrm{(Pb1Pb2)(\mu\text{-}O^iPr)_2}$, and $\mathrm{(Pb2Zr3)(\mu\text{-}O^iPr)}$ (where O16 $\neq$ O12 = O20) groups and $\mathrm{Zr(t\text{-}O^iPr)}$. The only remaining fluxionality implied by this is rotation of $\mathrm{Zr(t\text{-}O^iPr)}$ groups around the Zr3−Pb2 vector to yield a time-averaged C_3 axis for the $\mathrm{ZrPb2(O^iPr)_6}$ unit. At 25 °C in toluene-d_8, the coalesced ^{1}H NMR spectrum shows only one sharp doublet (at 1.39 ppm) for the methyl region and a very broad resonance (near 5.0 ppm) for the methine protons.

Since $\mathrm{Pb(O^iPr)_2}$ is a sparingly-soluble compound,[9] there is no possibility that the ^{1}H NMR signals are those of the separated molecules $\mathrm{PbZr(O^iPr)_6}$ and $\mathrm{Pb(O^iPr)_2}$. Indeed, our results show that $\mathrm{PbZr(O^iPr)_6}$ *solubilizes* $\mathrm{Pb(O^iPr)_2}$ in a nondestructive manner.[13,15]

The ^{207}Pb NMR spectrum of $\mathrm{Pb_4Zr_2(O^iPr)_{16}}$ in toluene at 104 MHz shows two lines (950 and 804 ppm) of equal intensity at −20 °C. These broaden by −10 °C, are almost undetectably broad at 25 °C, and have coalesced into one extremely (∼50 ppm half-width) broad line centered on 875 ppm at +55 °C. There is thus lead site exchange concurrent with the $\mathrm{O^iPr}$ site exchange. Perhaps the simplest mechanism for the lead site exchange is scission of the central (asymmetric) $\mathrm{Pb_2(O^iPr)_2}$ group, to yield a monomer (eq 5) which either has symmetry-related lead centers or itself executes rapid site exchange between inequivalent lead environments. Even if eq 5 is operative, K for this equilibrium must be very small since the +55 °C ^{207}Pb chemical shift is the average of the −20 °C chemical shifts; any dissociated product would thus have less than a 5% population.

$$\mathrm{Pb_4Zr_2(O^iPr)_{16}} \rightleftharpoons \mathrm{2Pb_2Zr(O^iPr)_8} \qquad (5)$$

$\mathrm{Pb_2Zr_4(O^iPr)_{20}}$. The solid-state structure of $\mathrm{Pb_2Zr_4(O^iPr)_{20}}$ is rigorously centrosymmetric (Figure 2) and is remarkably similar to that of $\mathrm{Pb_4Zr_2(O^iPr)_{16}}$. Its structure can be formally derived from its lead-rich analog ($\mathrm{Pb_4Zr_2(O^iPr)_{16}}$) by replacing the $\mathrm{Pb(2)(O^iPr)_2}$ units with $\mathrm{Zr(O^iPr)_4}$ units on either side of the central $\mathrm{Pb_2(O^iPr)_4}$ core. Thus, the μ-$\mathrm{O^iPr}$ linking Pb2 to Zr2 is part of a $\mathrm{Zr_2(O^iPr)_9}$ face-shared bioctahedron. The octahedron around Zr2 is somewhat distorted, since the O8−Zr2−O24 axis is bent (149.1(8)°). However, the Zr2, O12, O16, O20, O28 unit is rigorously coplanar (angles sum to 360°). In contrast, the Zr3 center is closer to octahedral with a O24−Zr3−O32 angle of 157.2(8)° and four other oxygens coplanar (angles sum to 358°). The Ot−Zr2−O8 angles (97.8(9) and 98.9(9)°) are smaller than the Ot−Zr3−O32 angles (99.5(9) and 100.3(9)°). As expected, bond lengths to terminal $\mathrm{O^iPr}$ ligands on Zr3 (1.89(2)−1.97(2) Å) and Zr2 (1.93(2) Å) are shorter than those to bridging ligands (2.16(2)−2.27(2) Å).

In contrast to $\mathrm{Pb_4Zr_2(O^iPr)_{16}}$, the six metals in $\mathrm{Pb_2Zr_4(O^iPr)_{20}}$ are distorted from planarity (Figure 3), allowing one of the μ-$\mathrm{O^iPr}$ ligands (between Zr centers) to approach Pb1 within (a weak) bonding distance (O28−Pb1 = 2.72(2) Å). This distance is markedly longer than any other Pb−O bond in the molecule (2.24(2)−2.43(2) Å) but is shorter than the Pb1−O20 distance (3.00(2) Å). Considering O28 as occupying a coordination site, Pb1 is four-coordinate and pseudo trigonal bipyramidal with O28 and O4′ axial (O28−Pb1−O4′ = 167.3(9)°) and O4 and O8 equatorial (O4−Pb1−O8 = 86.0(8)°). The remaining equatorial site is vacant. This Pb1/O28 interaction causes the Pb1/O4′ bond to lengthen, so that the central $\mathrm{Pb2(\mu\text{-}O^iPr)_2}$ unit here is asymmetric (Figure 3 and its caption); such asymmetry is absent in $\mathrm{Pb_4Zr_2(O^iPr)_{16}}$.

Interconversion of $\mathrm{Pb_4Zr_2(O^iPr)_{16}}$ and $\mathrm{Pb_2Zr_4(O^iPr)_{20}}$. Conversion of $\mathrm{Pb_4Zr_2(O^iPr)_{16}}$ to its zirconium-rich analog, $\mathrm{Pb_2Zr_4(O^iPr)_{20}}$, can be achieved by reaction with $\mathrm{Zr(O^iPr)_4}$ (eq 6).

$$\mathrm{Pb_4Zr_2(O^iPr)_{16}} + \mathrm{6Zr(O^iPr)_4} \xrightarrow{\Delta} \mathrm{2Pb_2Zr_4(O^iPr)_{20}} \qquad (6)$$

This reaction requires heating to 80 °C for approximately 1 h, similar to the synthesis of $\mathrm{Pb_2Zr_4(O^iPr)_{20}}$ from its constituent alkoxides. Likewise, $\mathrm{Pb_2Zr_4(O^iPr)_{20}}$ can be converted to the lead-rich species (eq 7) by addition of $\mathrm{[Pb(O^iPr)_2]}_n$ with

$$\mathrm{Pb_2Zr_4(O^iPr)_{20}} + (6/n)\mathrm{[Pb(O^iPr)_2]}_n \xrightarrow{\Delta} \mathrm{2Pb_4Zr_2(O^iPr)_{16}} \qquad (7)$$

subsequent heating at 80 °C for a short period of time. All reactions are based on NMR evidence, and products are obtained in >80% yield.

Titanium Analogs. Attempts were made to synthesize heterometallic species of formula $\mathrm{M}_x\mathrm{Ti}_y\mathrm{(OR)}_{2x+4y}$ (M = $\mathrm{Sn^{II}}$, $\mathrm{Pb^{II}}$; R = ^{i}Pr, ^{t}Bu) in ether. The general reaction used (eq 8)

$$\mathrm{M[N(SiMe_3)_2]_2} + \mathrm{Ti(OR)_4} + \mathrm{2HOR} \rightarrow \mathrm{M(OR)_2} + \mathrm{Ti(OR)_4} + \mathrm{2HN(SiMe_3)_2} \qquad (8)$$

resulted in the *in situ* formation of $\mathrm{M(OR)_2}$, which did *not* react with $\mathrm{Ti(OR)_4}$ as determined by NMR spectroscopy. Only the resonances of the unreacted starting materials were observed even after gentle heating for short periods of time. This result is most apparent when M = Pb and OR = $\mathrm{O^iPr}$, as $\mathrm{[Pb(O^iPr)_2]}_n$ precipitates from solution, in contrast to its being solubilized by $\mathrm{Zr(O^iPr)_4}$.

Sn/Zr/$\mathrm{O^iPr}$. Changing to a smaller divalent metal (eq 9) changes the behavior in the isopropoxide case to that seen for both $\mathrm{M^{II}/Zr/O^tBu}$ alkoxides: a 1:1 heterometallic alkoxide is

$$\mathrm{Zr_2(O^iPr)_8(^iPrOH)_2} + \mathrm{2Sn[N(SiMe_3)_2]_2} + \mathrm{2\,^iPrOH} \rightarrow \mathrm{2SnZr(O^iPr)_6} \qquad (9)$$

formed. This colorless waxy solid shows two alkoxide environments by ^{1}H and ^{13}C NMR spectroscopy at 25 °C in benzene and one Sn environment by ^{119}Sn NMR spectroscopy at 25 °C in toluene. $\mathrm{SnZr(O^iPr)_6}$ sublimes intact (^{1}H NMR evidence) at 40 °C and 10^{-2} Torr. This represents a major improvement in volatility upon reduction in molecular weight (compared to $\mathrm{SnZr(O^tBu)_6}$) of only 84 amu. The mass spectrum of SnZr-

---

(15) Compare to formation of an oxo alkoxide: Daniele, S.; Papiernik, R.; Hubert-Pfalzgraf, L. G.; Jagner, S.; Håkansson, M. *Inorg. Chem.* **1995**, *34*, 628.

$(O^iPr)_6$ also shows that sublimation occurs intact; the molecular ion ($m/e = 564$) is observed in the vapor phase.

Discussion

$PbZr(O^tBu)_6$ and $SnZr(O^tBu)_6$. In replacing Pb with Sn, we sought to find a heterometallic species with properties differing from those of $PbZr(O^tBu)_6$. Instead, we found that the Sn analog had nearly identical physical and spectral properties. One of their similarities is that by NMR spectroscopy each species exhibits one environment for its divalent metal. Assuming that these species are static (neither show significant broadening in their divalent metal NMR spectrum by -30 °C in toluene), their metal, ^1H, and ^{13}C NMR spectra can be stucturally diagnostic.

Although the coordination number of Pb in lead-containing alkoxides has not been observed to correspond well with the ^{207}Pb chemical shift,[16] some correlations have been made for chemical shifts of tin-containing alkoxides in ^{119}Sn NMR spectroscopy.[17] As the coordination number increases, the chemical shift moves upfield. Thus, an *increase* of 1 in coordination number usually results in a shift ~100−150 ppm upfield.[17] $SnZr(O^tBu)_6$ displays one resonance at -234 ppm, which is further *downfield* than that found for $Sn(O^tBu)_4$ (-371.4 ppm), a four-coordinate monomer both in the solid state[18] and in solution.[19] This resonance (234 ppm), however, is further *upfield* than that of $Sn(OC^tBu_3)_2$ (-162.9 ppm), a two-coordinate monomer in the solid state.[8a] By comparison, the chemical shift of $Sn(\mu\text{-}O^tBu)_3Cd(\mu\text{-}O^tBu)_3Sn$ (-225 ppm), which has three-coordinate tin atoms in the solid state,[20] is quite similar to that of $SnZr(O^tBu)_6$. This leads to the conclusion that the coordination number of tin in $SnZr(O^tBu)_6$ is 3, lending further support for this species being monomeric in solution. The similar physical and spectroscopic observations are also consistent with $PbZr(O^tBu)_6$ being monomeric in solution.

The presence of a lone pair on the divalent metal of $M^{II}Zr(OR)_6$ might allow these species to act as Lewis bases toward electrophilic compounds if the lone pair were sp^3-hybridized. Certain examples[21] show that the metal of tin alkoxides can act as an electron donor to a transition metal carbonyl compound. However, our $M^{II}Zr(OR)_6$ species do not react with Lewis acids such as BPh_3, BEt_3, and $AlMe_3$. We believe that the divalent metal lone pair has more s-orbital character and is thus not stereochemically-active. This is further supported by the geometry of Pb1 in $Pb_4Zr_2(O^iPr)_{16}$. The O−Pb−O angles (71.2(6)−90.2(7)°) are indicative of the p character of the bonding orbitals of Pb.

$Pb_4Zr_2(O^iPr)_{16}$ and $Pb_2Zr_4(O^iPr)_{20}$.[22,23] An attempt to synthesize the $PbZr(O^tBu)_6$ analog with O^iPr ligands produces two species of differing metal stoichiometries. These species are similar in solubility, molecular weight, and related solid-state structure. Indeed they *both* adopt a rare, serpentine structure[24] where the potentially spiro metals (Pb1 in both structures) are of low coordination number. The reason for this is not fully understood; however, Pb^{II} often has a low coordination number (i.e., 3 or 4).[9,20] The "open" structure is the result of the preference for a lower (than six) coordination number Pb1.

These $Pb/Zr/O^iPr$ compounds display interesting properties in solution. Placing these together in a 1:1 ratio in benzene shows no sign of fluxionality (25 °C, 300 MHz) which would be caused by facile (rapid) interconversion. Rational synthesis of either compound can be accomplished by simply heating a stoichiometric mixture of $[Pb(O^iPr)_2]_n$ and $Zr(O^iPr)_4$ in benzene for an hour or less. Yields obtained are quite high (>80%). More remarkably, one species can be converted to the other by simply adding the appropriate metal alkoxide.

$Pb_4Zr_2(O^iPr)_{16}$. While this molecule is fluxional at room temperature, at -60 °C, five chemical environments in the methine region are observed of relative intensity 2:2:2:4:6 attributed to alkoxides a, b, c, d, and e, respectively (structure **B**). Although the first four environments are consistent with those found in the solid-state structure, environment e should consist of two different resonances of integration 2:1 for the two alkoxides *trans* to alkoxide d and the one *trans* to alkoxide c. These are not decoalesced or resolved, apparently due to a small chemical shift difference. The integration ratios observed in solution are in good agreement with the solid-state structure. Although the longest bond in the structure is the bridge from the $PbZr(O^iPr)_6$ unit to the $Pb_2(O^iPr)_2$ unit, it is certain that this molecule remains intact in solution since the $[Pb(O^iPr)_2]_n$ species is insoluble in benzene and no solid material was observed to precipitate from solution.

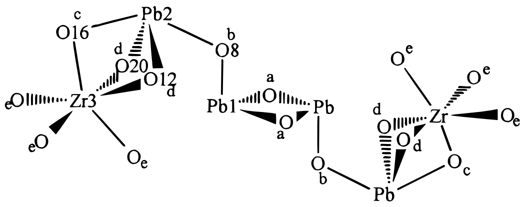

B

Frequently, when two Zr metals are present in a bimetallic alkoxide species, they are six-coordinate centers which are either edge-[25] or face-shared.[26] In $Pb_4Zr_2(O^iPr)_{16}$, the Zr metals are six-coordinate but do not face-share with each other. Instead, the Zr centers are found on opposite ends of the molecule and are face-sharing with lead. To our knowledge, this is the first crystallographically-characterized homoleptic alkoxide moiety where the Zr centers are not directly linked into a $Zr_2(OR)_9^-$ unit.

$Pb_2Zr_4(O^iPr)_{20}$. The structure of $Pb_2Zr_4(O^iPr)_{20}$ is strikingly similar to that of $Pb_4Zr_2(O^iPr)_{16}$. However, the difference between these two, besides metal stoichiometry, is the coordination number at Pb1. In the latter, it is three-coordinate, whereas

---

(16) Papiernik, R.; Hubert-Pfalzgraf, L. G.; Massiani, M. C. *Polyhedron* **1991**, *10*, 1657.

(17) Hampden-Smith, M. J.; Wark, T. A.; Brinker, C. J. *Coord. Chem. Rev.* **1992**, *112*, 81.

(18) Hampden-Smith, M. J.; Wark, T. A.; Rheingold, A.; Huffman, J. C. *Can. J. Chem.* **1991**, *69*, 121.

(19) (a) Bradley, D. C.; Caldwell, E. A. U.; Wardlaw, W. *J. Chem. Soc. A* **1957**, 4775. (b) Marie, J.-C. *Ann. Chim.* **1961**, 969.

(20) Veith, M.; Hans, J.; Stahl, L.; May, P.; Huch, V.; Sebald, A. *Z. Naturforsch.* **1991**, *46B*, 403.

(21) (a) Veith, M.; Kunze, K. *Angew. Chem., Int. Ed. Engl.* **1991**, *30*, 95. (b) Veith, M.; Hans, J. *Angew. Chem., Int. Ed. Engl.* **1991**, *30*, 879. (c) Veith, M.; Käfer, D.; Koch, J.; May, P.; Stahl, L.; Huch, V. *Chem. Ber.* **1992**, *125*, 1033.

(22) Teff, D. J.; Huffman, J. C.; Caulton, K. G. *Inorg. Chem.* **1995**, *34*, 2491.

(23) $Pb_2Zr_4(O^iPr)_{20}$ was reportedly synthesized, but no details were given: Mehrotra, R. C.; Singh, A.; Sogani, J. *Chem. Rev.* **1994**, *94*, 1643.

(24) Another rare example of a serpentine metal complex is $Mo_6O_{10}(O^iPr)_{12}$: Chisholm, M. H.; Folting, K.; Huffman, J. C.; Kirkpatrick, C. C. *Inorg. Chem.* **1984**, *23*, 1021.

(25) (a) $[Zr(O^iPr)_8(HO^iPr)_2]$: Vaartstra, B. A.; Huffman, J. C.; Gradeff, P. S.; Hubert-Pfalzgraf, L. G.; Daran, J.-C.; Parraud, S.; Yunlu, K.; Caulton, K. G. *Inorg. Chem.* **1990**, *29*, 3126. (b) $[PbZr_2(O)(OOCCH_3)_2(OCH_2CH_3)_6]_2$: Ma, L.; Payne, D. A. *Chem. Mater.* **1994**, *6*, 875.

(26) (a) $[KZr_2(O^iPr)_9]$: Vaartstra, B. A.; Streib, W. E.; Caulton, K. G. *J. Am. Chem. Soc.* **1990**, *112*, 8593. (b) $[(\mu\text{-}Cl)(CdZr_2(O^iPr)_9]_2$: Sogani, J.; Singh, A.; Bohra, R.; Mehrotra, R. C.; Nottemeyer, M. *J. Chem. Soc., Chem. Commun.* **1991**, 738.

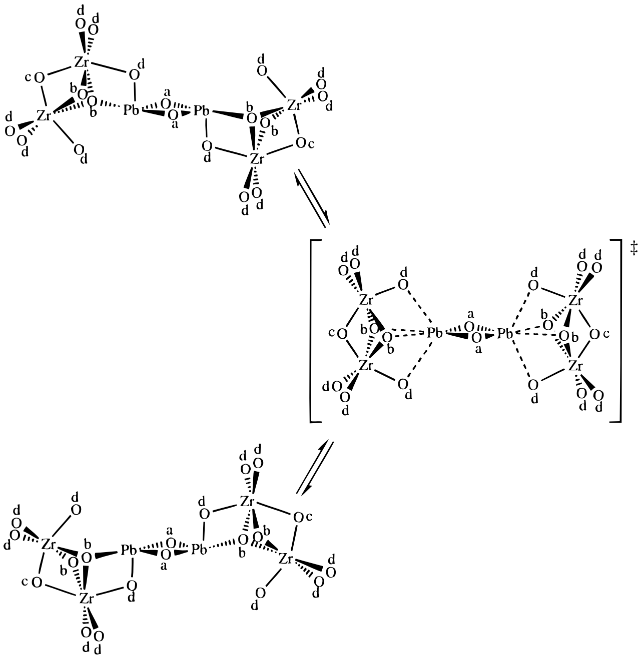

Figure 4. Proposed fluxional process and consequent site-averaging for $Pb_2Zr_4(O^iPr)_{20}$. O^iPr is indicated by “O”.

in the former, it is four-coordinate, due to O28 adopting a μ_3-bridging role. The six metals deviate from planarity (Figure 3), and this further differentiates the structure from that of $Pb_4Zr_2(O^iPr)_{16}$.

The simple room-temperature ^1H NMR spectrum of $Pb_2Zr_4(O^iPr)_{20}$ can be decoalesced to four distinct peaks in the methine region at low temperature. The integration ratio is 2:4:2:12 and does not correspond to environments in the solid-state structure, unless there is still fluxionality in solution at low temperature (i.e., there are too few environments seen by NMR). We propose that a possible mechanism (Figure 4) that would generate environments a, b, c, and d, respectively, involves “rocking” the $Zr_2(O^iPr)_9$ unit back and forth slightly. Alternatively, this rocking could involve only one $Zr_2(O^iPr)_9$ group at a time. The only remaining fluxionality is that which relates the d alkoxides.

$$Sn[N(SiMe_3)_2]_2 + Zr_2(O^iPr)_8(HO^iPr)_2 \rightarrow SnZr(O^iPr)_6 + Zr(O^iPr)_4 + 2HN(SiMe_3)_2 \quad (10)$$

$SnZr(O^iPr)_6$. Attempts were made to isolate higher nuclearity complexes, as in $Pb_xZr_y(O^iPr)_{2x+4y}$ ($x = 2, 4$; $y = 4, 2$), using the smaller (than Pb) tin atom. One analog, $[SnZr_2(O^iPr)_{10}]_n$ was reportedly synthesized via salt metathesis.[27] However, we have made two attempts to isolate this compound by other means (eqs 10 and 11). Both resulted in the known

$$Sn(O^iPr)_2 + 2Zr(O^iPr)_4 \xrightarrow{\Delta} SnZr(O^iPr)_6 + Zr(O^iPr)_4 \quad (11)$$

products $SnZr(O^iPr)_6$ and $Zr(O^iPr)_4$ (^1H and ^{13}C NMR evidence). Thus, in changing to a smaller metal *and* ligand set, we retain the 1:1 metal stoichiometry observed for the O^tBu compounds.

The volatility of $SnZr(O^iPr)_6$ is remarkably enhanced (40 °C and 10^{-2} Torr) compared to that of the 1:1 O^tBu species (120 °C and 10^{-2} Torr), probably arising from a decrease in molecular weight. Also, it is a monomer in the gas phase as determined by its mass spectrum.

Scheme 1

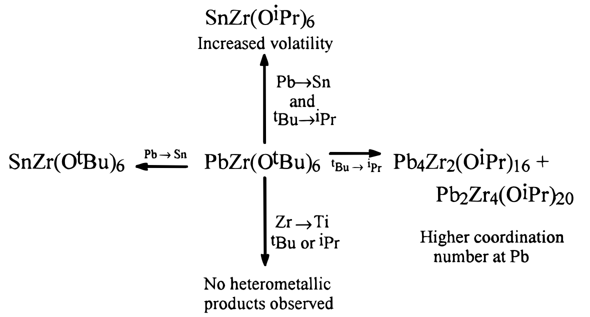

Examination by ^{119}Sn NMR produced one resonance at −260 ppm. This value is very similar to that of $SnZr(O^tBu)_6$ (−234 ppm), suggesting that the tin atom of $SnZr(O^iPr)_6$ is also three-coordinate, and thus the compound is monomeric in solution, as well as in the gas phase.

Titanium Analogs. When $M^{II}(OR)_2$, generated *in situ* from $M[N(SiMe_3)_2]_2$ and ROH, is added to the corresponding $Ti(OR)_4$ ($R = {}^iPr, {}^tBu$) at 25 °C in Et_2O, there is no evidence for adduct formation. ^1H and ^{13}C NMR indicated that chemical shifts of only the unreacted starting materials were present in solution. The lack of reaction is particularly evident in the case of $Pb(O^iPr)_2$, since this polymeric and insoluble compound remains undissolved,[28] in contrast to its being “solubilized” by $Zr(O^iPr)_4$. We believe the lack of reactivity seen for these titanium alkoxides is due to the smaller size of titanium and its consequent inability to adopt the high coordination number found in heterometallic alkoxides. When the size of the metal is decreased, the coordination sphere becomes more congested, and M−O dative bonds are sacrificed to relieve this congestion. Therefore, six-coordinate Ti is not achieved because of the steric requirements of the ligands, even in the case of O^iPr. This point may be further illustrated by the fact that Zr readily forms an isolable alcohol adduct, $Zr_2(O^iPr)_8(HO^iPr)_2$,[25a] whereas Ti does not.[29]

Conclusions

The influence of M^{II}, M^{IV}, and R in this study is succinctly summarized in Scheme 1. When M^{II} is Pb and R is made smaller, aggregation can increase via enhanced bridging to lead, which accepts a higher coordination number. When both R and M^{II} are made smaller, these two factors compensate each other and the stoichiometry remains 1:1:6. When M^{II} alone is made smaller, Sn can still tolerate three O^tBu ligands, and so a 1:1:6 compound is still produced. However, the size difference between Zr and Ti is apparently so great that $PbTi(O^tBu)_6$, with six O^tBu groups around Ti, is not formed under conditions used here. Moreover, no product forms, even when using the smaller isopropoxide ligand. However, part of the reason here may lie in the degree of aggregation of $[Ti(OR)_4]_n$. That is, no heterometallic adduct may form because the Lewis acidity of these binary titanium alkoxides is low due to alkoxide bridging and higher coordination number.

Acknowledgment. This work was supported by the Department of Energy.

Supporting Information Available: Tables of full crystallographic details, fractional coordinates, and anisotropic thermal parameters (5 pages). Ordering information is given on any current masthead page.

IC951413H

---

[27] Mathur, S.; Singh, A.; Mehrotra, R. C. *Polyhedron* **1993**, *12*, 1073.

[28] Refluxing $[Pb(O^iPr)_2]_n$ in toluene in the presence of $Ti(O^iPr)_4$ has been shown to form a heterometallic oxo alkoxide. See ref 15.

[29] Bradley, D. C.; Mehrotra, R. C.; Gaur, D. P. *Metal Alkoxides*; Academic: New York, 1978.